PCCP

ROYAL SOCIETY OF CHEMISTRY

PAPER

View Article Online
View Journal | View Issue

Cite this: *Phys. Chem. Chem. Phys.*, 2026, **28**, 3316

Riboflavin – understanding the dynamics and interactions of the triplet state

Marek Scholz, Jan Moučka, Jakub Pšenčík, Jan Hála and Roman Dědic *

Riboflavin, a water-soluble vitamin and important nutrient found in many foods, also functions as an effective photosensitiser, with a singlet oxygen quantum yield of 0.54. This makes it relevant not only for photodynamic therapy (PDT) but also as a contributor to light-induced degradation of food and beverages. However, literature reports on its triplet and singlet oxygen dynamics remain inconsistent. We show that in phosphate buffered water, riboflavin exhibits a triplet state lifetime of 3.2 μs and a singlet oxygen lifetime of 3.7 μs, unusually close values that require careful kinetic analysis for a correct interpretation. Contrary to some assumptions, we find that sodium azide efficiently quenches riboflavin triplets (rate constant 4×10^9 M^{-1} s^{-1}), far exceeding the quenching rate of azide for singlet oxygen. In contrast, we demonstrate that the quenching of singlet oxygen by riboflavin is negligible under typical conditions in H_2O. We also report pronounced delayed fluorescence (DF) of riboflavin in air-saturated samples, attributed to the singlet oxygen feedback mechanism. Finally, we discuss how the DF signal can be used to reveal energy transfer efficiency to other sensitisers, such as aluminium phthalocyanine, where we demonstrate a dominant role of the triplet–triplet transfer mechanism.

Received 8th October 2025,
Accepted 20th December 2025

DOI: 10.1039/d5cp03884g

rsc.li/pccp

1 Introduction

Riboflavin (Rf, vitamin B_2) is a crucial micronutrient found in a variety of foods (*e.g.* milk, eggs, and green vegetables) and is essential for normal cellular function. In living organisms, riboflavin performs its biochemical functions by being converted to the coenzymes flavin mononucleotide (FMN) and flavin adenine dinucleotide (FAD) that participate in numerous metabolic reactions.[1]

Beyond its nutritional importance, riboflavin has attracted interest due to its photochemical properties. It is a yellow orange aromatic isoalloxazine compound that strongly absorbs ultraviolet and visible light (with absorption peaks near 224, 268, 373, and 445 nm) and emits fluorescence around 535 nm with a quantum yield of approximately 0.3.[2]

Upon exposure to light, riboflavin can be excited to higher energetic states and engage in photochemical reactions involving oxygen. Its photosensitivity leads to the oxidative degradation of foods and beverages after exposure to light, leading to off-flavour of dairy products or beer.[3,4] On the other hand, riboflavin is one of the prominent endogenous chromophores in biological tissues that can produce reactive oxygen species (ROS) under illumination, which has been explored in applications such as pathogen inactivation and photodynamic therapy (PDT). Riboflavin and its derivatives have been studied as potential photosensitisers for the treatment of skin diseases and cancers, since they are nontoxic water-soluble vitamins that can generate cytotoxic singlet oxygen when activated by light.[2] A group of flavoproteins producing singlet oxygen with high quantum yield was developed: SOPPs with FMN as a chromophore[5,6] or miniSOG-Q103L using Rf.[7]

Upon illumination, riboflavin in water solutions forms a triplet state ^{3}Rf* with a quantum yield of 0.6–0.7,[8,9] which then efficiently interacts with the surrounding oxygen to form singlet oxygen ($^1O_2$) with a quantum yield of 0.54 ± 0.07 in aerated H_2O solutions.[9] † This finding underscores that flavins, such as riboflavin and FMN, can be efficient type II photosensitizers under physiological conditions that can be used in photodynamic therapy or to photodeactivate viruses and bacteria.[7,11–16]

However, riboflavin also has significant drawbacks that complicate its use in photodynamic applications. It has a limited solubility in water: on the order of 0.08 g L^{-1} (only up to 200 μM) at room temperature and neutral pH.[17,18] ‡ Riboflavin also undergoes rapid photodegradation after illumination under both aerobic and anaerobic conditions, primarily involving cleavage and modification of its ribityl side chain,

Charles University, Faculty of Mathematics and Physics, Department of Chemical Physics and Optics, Prague, The Czech Republic.
E-mail: Roman.Dedic@matfyz.cuni.cz; Tel: +420 95155 1234

† For FMN, singlet oxygen quantum yields of 0.49 ± 0.05 in H_2O and 0.65 ± 0.04 in D_2O have been reported.[5,10]

‡ Notably, the phosphorylated ribityl side chain in FMN dramatically improves solubility in water, while preserving the isoalloxazine chromophore intact, leaving many of the photophysical properties very similar to riboflavin.[19]

producing a series of photoproducts, such as lumichrome and lumiflavine.[20]

Because riboflavin both generates ROS and is susceptible to them, a pertinent question has been whether riboflavin can act as an antioxidant (*i.e.* a quencher of singlet oxygen or other ROS) in addition to being a photosensitiser. Some earlier studies claimed that riboflavin could physically quench singlet oxygen at almost diffusion-controlled rates (approx. 10^9–10^{10} M^{-1} s^{-1}), implying that riboflavin could protect against oxidative damage by scavenging $^1O_2$.[21,22] However, in those works, the rate constant was determined only indirectly by measuring degradation of riboflavin and depletion of oxygen. The authors also came to the wrong conclusion that sodium azide quenches only singlet oxygen and not riboflavin triplets (see the discussion below). In contrast, direct measurements based on singlet oxygen phosphorescence lifetimes yielded much lower quenching rates – Chacon *et al.*[8] reported 6×10^7 M^{-1} s^{-1} in CH_3OD, but they did not provide much detail and did not show a Stern–Volmer plot. Recently, a more detailed and accurate analysis by Insińska-Rak *et al.*[19] yielded even lower values; an estimate of 2×10^6 M^{-1} s^{-1} was obtained from Rf measurements in D_2O and the value of 1.7×10^5 M^{-1} s^{-1} was obtained for FMN. The causes of the discrepancies with the previous results are discussed therein. In other words, riboflavin is actually a rather poor singlet oxygen quencher in aqueous solutions, especially compared to dedicated antioxidants. Previous reports of riboflavin's high quenching ability may have stemmed from experimental artefacts or incorrect interpretations of experimental data. However, determining the quenching rate in H_2O remains a challenge.

A related issue arises when considering sodium azide (NaN_3) as a tool in riboflavin photochemical experiments. Sodium azide is a well-known selective quencher of singlet oxygen: it reacts with $^1O_2$ and is therefore often used to distinguish type II (singlet oxygen-mediated) photoreactions from other pathways.[23,24] The azide anion typically does not significantly quench the triplet excited states of most common photosensitisers; for example, in porphyrin and dye systems, NaN_3 scavenges $^1O_2$ but does not interact with the triplet state of the sensitiser.[25] Consequently, many riboflavin photochemical studies have used azides to confirm singlet oxygen involvement, assuming that NaN_3 only removes $^1O_2$ and leaves the triplet state of Rf intact.[21,26–28] Given the widespread use of NaN_3 as a 'specific' singlet oxygen quencher in riboflavin photosensitisation studies, it is desirable to determine whether azides truly leave the riboflavin triplet state unaffected and, if not, to determine the magnitude of its quenching effect.

A common experimental method to study the photosensitisation process is the detection of weak singlet oxygen phosphorescence around 1270 nm, which typically follows a biexponential rise decay in the form of

$$I(t) = A\left[\exp\left(-\frac{t}{\tau_1}\right) - \exp\left(-\frac{t}{\tau_2}\right)\right], \quad (1)$$

with $\tau_1 > \tau_2$. The rise time τ_2 usually corresponds to the triplet lifetime (τ_T), while τ_1 corresponds to the lifetime of $^1O_2$ (τ_Δ). Interestingly, the lifetime of the triplet state of riboflavin in aerated solutions based on H_2O has been reported to be about (3.2 ± 0.5) μs,[9] which is longer than that of many other PDT-relevant photosensitisers (*e.g.* porphyrin TPPS4 has a triplet lifetime of 1.8 μs).[25] The lifetime of singlet oxygen in unquenched H_2O-based solutions is typically 3.5–4.0 μs,[29,30] which is close to the triplet lifetime of riboflavin. This makes the analysis of singlet oxygen luminescence kinetics challenging because the fitting of the data with two close lifetimes is usually ill-conditioned and could lead to large errors or misleading interpretations. We address this issue in this report.

Riboflavin itself has been reported to have weak phosphorescence around 620 nm at low temperatures in rigid deoxygenated media.[31] However, we note an interesting luminescence phenomenon that has been observed in solutions of various photosensitisers at room temperature but remains unexplored for riboflavin: delayed fluorescence resulting from singlet oxygen feedback (SOFDF). In several water-soluble photosensitisers (such as rose bengal, eosin and porphyrins such as protoporphyrin IX), weak delayed emission can be detected after prompt fluorescence has decayed, which is attributable to the so-called singlet oxygen feedback delayed fluorescence mechanism.[25,32,33] In this process, some of the singlet oxygen molecules generated by the triplet sensitiser collide with another triplet and transfer their energy back to the sensitiser, reexciting it to an excited singlet state, which then emits fluorescence at a delayed time. This can be summarised as a series of reactions:

$$^3PS^* + {}^3O_2 \rightarrow {}^1PS + {}^1O_2{}^*$$

$$^1O_2{}^* + {}^3PS^* \rightarrow {}^3O_2 + {}^1PS^*$$

$$^1PS^* \rightarrow {}^1PS + \text{photon}$$

Similar to the $^1O_2$ kinetics, the SOFDF kinetics has a rise-decay profile with two lifetimes that are related to the $^1O_2$ and $^3Rf^*$ lifetimes (τ_Δ and τ_T, respectively) by the equations[34]

$$\tau_{rise} = \tau_T/2, \quad \tau_{decay} = \frac{\tau_T \tau_\Delta}{\tau_T + \tau_\Delta} \quad (2)$$

This phenomenon provides a unique optical signature of $^1O_2$ and an alternative way to monitor triplet-sensitised processes. To the best of our knowledge, delayed fluorescence from riboflavin in solution has not been reported in the literature so far. The energy of the riboflavin triplet is around 193 kJ mol^{-1},[31] while its excited singlet has an energy of approximately 226 kJ mol^{-1}. The singlet–triplet energy gap of 40 kJ mol^{-1} is lower than the energy of the $^1O_2$ molecule (94 kJ mol^{-1}), and therefore such back-energy transfer and delayed emission are feasible in riboflavin. Investigating whether riboflavin can exhibit delayed emission would further elucidate the excited state dynamics of this vitamin and could open up new detection methods for riboflavin's photoreactivity.

In this work, we investigate in detail the triplet state dynamics of riboflavin and determine the corresponding

lifetimes of excited states. We also explore the effect of sodium azide on the excited triplet state of riboflavin, measuring the quenching rate constant. Furthermore, we revisit the potential of riboflavin to quench singlet oxygen in solutions based on H_2O. Next, we searched for any observable delayed fluorescence or phosphorescence of riboflavin in water at room temperature, as these signals could provide additional insight into the dynamics of the riboflavin triplet state. Building on this, we study the energy transfer from riboflavin to another photosensitiser aluminium phthalocyanine. Through this study, our objective is to provide deeper insight into the photochemistry of riboflavin, knowledge that is important both for fundamental photochemical understanding and for practical application of this vitamin in photodynamic systems and the food industry.

2 Materials

Riboflavin (Sigma-Aldrich R9504, purity $\geq$98%) was dissolved in Biosera Dulbecco H_2O-based phosphate buffered saline (LM-S2041, pH 7.4) at a concentration of 200 μM for stock solutions. This was further diluted to the target concentrations. 50 μM was used for most experiments. Aluminium phthalocyanine tetrasulphonate (Frontier Scientific, AlPcS-834, purity >95%) was also dissolved in the H_2O-based phosphate buffered solution at a concentration of 1 mM for the stock solution and further diluted to final concentrations, mainly 100 μM or lower. Throughout this work, H_2O-based buffer was used in all experiments with the exception of a single control experiment described in Section 4.5, in which riboflavin was dissolved in D_2O-based phosphate buffer prepared from a Sigma-Aldrich PBS tablet (P4417) and D_2O (Sigma-Aldrich 151882, 99.9 atom % D).

3 Methods

3.1 $^1O_2$ and DF detection (setup 1)

Weak infrared emission of singlet oxygen was detected using a gated infrared photomultiplier (Hamamatsu H12694-45). The samples were excited by ~5 ns pulses provided by the EKSPLA NT242 laser with a 1 kHz repetition rate. Luminescence was collected using an optical fibre and guided to the photomultiplier through a band-pass filter centred at 1274 nm with a bandwidth of 40 nm (Omega Optical). The signal from the photomultiplier was detected using a time-resolved counter (Becker & Hickl MSA300).

In the case of delayed fluorescence, the same excitation laser and time-resolved counter were used. In this setup, gated APD (laser components COUNT-100C-FC) was employed to detect the luminescence. A 562-nm band-pass filter with a bandwidth of 40 nm (Edmund Optics) was used for riboflavin emission, whereas a long-pass filter RG630 (Schott) plus a bandpass filter 692/40 nm were used for the emission of phthalocyanine.

Both the $^1O_2$ and the DF emission kinetics were fitted by two exponentials using the Python library lmfit.

3.2 Luminescence detection using a camera (setup 2)

The time-resolved spectra of prompt and delayed fluorescence were measured using a ns gated spectroscopic camera (Princeton Instruments PI-MAX 4) attached to the output of the inverted luminescence microscope Olympus IX73 through an imaging spectrograph (Princeton Instruments ARC-SP-2358). Excitation pulses were provided by the same laser as described previously.

3.3 Transient absorption (setup 3)

For measurements of transient absorption spectra, the samples were excited by laser pulses (~3 ns width, energy 0.5 mJ) from an optical parametric oscillator (EKSPLA PG122) pumped by a Q-switched Nd:YAG laser (EKSPLA NL303G/TH) at a 10 Hz repetition rate. Absorption was probed using a pulsed xenon lamp (PerkinElmer LS-1130-1) perpendicular to excitation. The transmitted light was spectrally resolved using an imaging spectrometer (Horiba Jobin-Yvon iHR320) and detected using an intensified gated camera (Roper Scientific PI-MAX 512RB). A series of spectra were acquired with an increasing delay after the excitation pulse. Global analysis[35] was used to extract individual spectral components and their corresponding lifetimes. When the xenon lamp is turned off, this setup also enables recording time-resolved spectra of the prompt and delayed fluorescence.[25]

4 Results and discussion

4.1 ^{3}Rf lifetimes

Transient absorption measurements were performed using 50 μM riboflavin in PBS-buffered H_2O with setup no. 3. Transient spectra were recorded at a series of delay times after the excitation pulse (Fig. 1). Upon excitation, a fraction of riboflavin molecules is promoted from the ground state (S_0) to the excited singlet state (S_1) and subsequently undergoes an intersystem crossing to the triplet state (T_1). The resulting spectra exhibit a

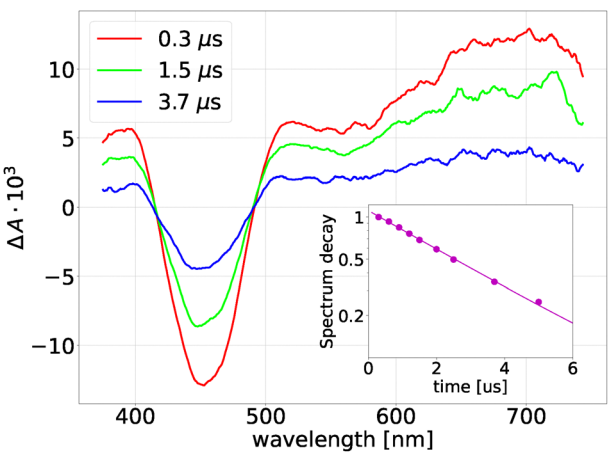

Fig. 1 Transient absorption spectra of riboflavin solution at different times after the excitation pulse show the ground state bleaching band around 450 nm accompanied by the triplet–triplet absorption bands in the red portion of the spectrum. Inset: Transient absorption spectrum decay.

prominent negative band centred at 450 nm, attributed to the depletion of riboflavin molecules in the ground state as they populate the T_1 state. Furthermore, a positive band in the range of 600–750 nm corresponds to absorption of ^{3}Rf*.[36] Global analysis[37] of time-resolved spectra revealed a single lifetime component that corresponds to the ^{3}Rf* lifetime, yielding $\tau_T = (3.1 \pm 0.1)$ μs.

4.2 $^1O_2$ kinetics in H_2O

The singlet oxygen phosphorescence kinetics of riboflavin in air-saturated PBS/H_2O were measured using setup no. 1 and analysed to extract the triplet state lifetime (τ_T) and the singlet oxygen lifetime (τ_Δ). The kinetic traces were fitted using a biexponential model (1), as shown in Fig. 2. In some cases, the fits converged to distinct lifetimes of $t_1 = (3.7 \pm 0.1)$ μs and $t_2 = (3.3 \pm 0.1)$ μs, while in other instances, the fits yielded nearly identical values for both components $t_1 \simeq t_2 \simeq 3.5$ μs, with differences as small as 0.02 μs. This behaviour requires further discussion.

Our measurements using other sensitisers (for example, porphyrins and eosin) in PBS/H_2O gave a consistent singlet oxygen lifetime of $\tau_\Delta = (3.8 \pm 0.1)$ μs and a triplet lifetime of ~2 μs.[25] Here, transient absorption measurements yielded a triplet state lifetime for riboflavin of $\tau_T = (3.1 \pm 0.1)$ μs. The proximity of the ^{3}Rf* and $^1O_2$ lifetimes presents a challenge in fitting the biexponential kinetics reliably. When the data are noisy and the rise and decay components are close, the sum of squared residuals becomes insensitive to variations in the parameters, often leading the minimisation routine to converge to local minima where $\tau_1 = \tau_2$, producing lifetime uncertainties exceeding 100%. These effects were confirmed by our *in silico* simulations: when τ_T and τ_Δ were closer than 0.6 μs, the fitting algorithm frequently converged to the misleading result $\tau_1 = \tau_2$.

When the rise and decay components of singlet oxygen kinetics are suspected to be strongly coupled, it is critical to proceed cautiously. An effective strategy is to fix one of the lifetimes using independent data, *e.g.*, fixing τ_T from transient absorption measurements, allowing for a more reliable estimation of τ_Δ during the fitting process. Alternatively, the singlet oxygen lifetime can be independently determined by performing measurements in oxygen-saturated PBS/H_2O. Under this condition, the riboflavin triplet state is rapidly quenched, effectively decoupling the two lifetimes and simplifying the fit. This approach yielded $\tau_\Delta = (3.65 \pm 0.10)$ μs and $\tau_T = (0.61 \pm 0.05)$ μs. Therefore, when studying the evolution of τ_T under varying conditions, fixing τ_Δ based on such independent measurements can help reduce cross-correlation artefacts and improve the robustness of the analysis.

Another possible approach is to perform experiments in D_2O, which leads to a dramatic increase in the $^1O_2$ lifetime from about 3.7 μs to 69 μs.[19] This decouples the $^1O_2$ lifetime from the ^{3}Rf* lifetime and allows for a more reliable fitting of the τ_T lifetime. Westberg *et al.* showed that the triplet lifetime of a free FMN is equal to 3.2 μs in both H_2O and D_2O, and therefore the isotopic exchange did not significantly influence the triplet lifetime in that case, although they observed an isotopic exchange effect on τ_T for flavins bound to proteins.[5]

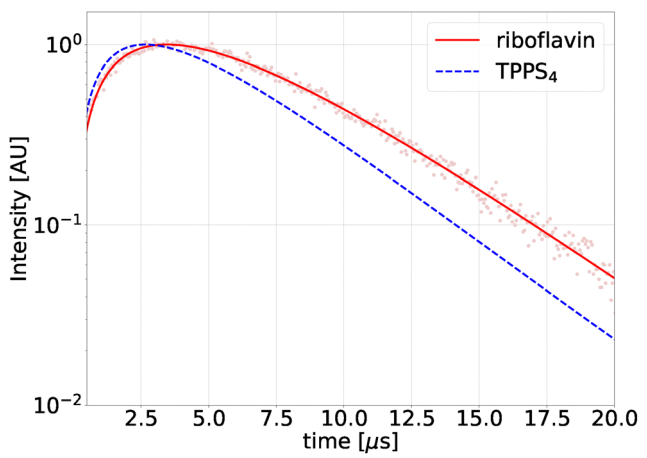

Fig. 2 Comparison of the $^1O_2$ luminescence kinetics photosensitized by riboflavin (red) and porphyrin $TPPS_4$ (blue). The slower rise of the red curve documents that the lifetime of ^{3}Rf* is significantly longer.

4.3 Riboflavin as an $^1O_2$ quencher

We performed a simplified version of the experiment reported by Ogilby's group,[19] but in H_2O instead of D_2O. The goal was to assess whether riboflavin can quench $^1O_2$ by observing changes in the phosphorescence lifetime of $^1O_2$. Aluminium phthalocyanine tetrasulfonate (AlPc) was used as a photosensitiser to produce $^1O_2$ due to its well-separated absorption spectrum from riboflavin, allowing selective excitation at wavelengths >600 nm. We used 605 nm excitation as a compromise between the absorption coefficient of AlPc and the power of the laser. In PBS buffered H_2O, AlPc alone (100 μM) produced $^1O_2$ with a measured lifetime of $\tau_\Delta = (3.72 \pm 0.04)$ μs and a triplet state lifetime of $\tau_T = (1.8 \pm 0.1)$ μs, corresponding to an overall $^1O_2$ decay rate of $K_0 = (2.69 \pm 0.03) \times 10^5$ s^{-1}, primarily due to vibrational deactivation through O–H bonds in water. Upon the addition of 133 μM riboflavin – similar to the conditions used by Ogilby's group – the $^1O_2$ lifetime remained unchanged within the experimental uncertainty ($\tau_\Delta = (3.70 \pm 0.05)$ μs, $K = (2.70 \pm 0.04)\ 10^5$ s^{-1}). Thus, the maximum possible change in the decay rate due to riboflavin is within the margin of error: $K_{q,max} = 8 \times 10^3$ s^{-1}. Given the riboflavin concentration of 1.33×10^{-4} M, this translates to an upper limit for the bimolecular quenching rate constant of $k_{q,max} = K_{q,max}/c = 6 \times 10^7$ M^{-1} s^{-1}, which is two orders of magnitude lower than the old diffusion-controlled estimates.[21,22]

It should be emphasised here that due to an inherently short $^1O_2$ lifetime in H_2O, the addition of riboflavin (even at concentrations close to the solubility limit) did not induce any statistically significant change in the $^1O_2$ lifetime. In terms of the bimolecular quenching rate, we can only conclude that the real value can be anywhere between zero and 6×10^7 M^{-1} s^{-1}. In this sense, our findings in H_2O are consistent with the recent results obtained in a detailed study by Ogilby's group:[19] $k_q \lesssim 2 \times 10^6$ M^{-1} s^{-1} for Rf in D_2O and $k_q = 1.7 \times 10^5$ M^{-1} s^{-1} for FMN. For comparison, the quenching rates by sodium azide,

amino acids such as histidine, or carotenoids are 2–4 orders of magnitude higher.[38–40]

In conclusion, even near its limit of solubility, riboflavin has a negligible effect on the removal of $^1O_2$ in aqueous systems and cannot be considered a significant quencher under these conditions.

4.4 NaN_3 quenches $^3Rf^*$

The quenching rate of $^3Rf^*$ by sodium azide was determined from time-resolved transient absorption spectroscopy, as described in Section 4.1. The decay kinetics of $^3Rf^*$ (50 μM) were measured at varying NaN_3 concentrations (0 mM, 0.1 mM, 0.2 mM and 0.3 mM), which yielded progressively shorter lifetimes of 3.1 μs, 1.41 μs, 0.87 μs and 0.66 μs, respectively. A control measurement with 5 mM NaN_3 showed a lifetime below 50 ns. Fig. 3 presents a Stern–Volmer plot of the inverse lifetimes $\left(\frac{1}{\tau}\right)$ *versus* azide concentration, showing a linear relationship according to the following equation:

$$\frac{1}{\tau} = \frac{1}{\tau_0} + k_q \cdot [NaN_3].$$

The slope gives a bimolecular quenching rate constant for riboflavin triplets

$$k_{q,T} = (4.0 \pm 0.1) \times 10^9\ M^{-1}\ s^{-1}.$$

An independent method based on singlet oxygen phosphorescence kinetics was also used to determine both the triplet quenching rate and the singlet oxygen removal rate. Measurements were performed for a series of NaN_3 concentrations (0–0.5 mM). Both the rise time (τ_T) and the decay time (τ_Δ) decreased with increasing azide concentration. For example, we obtained $\tau_T = 3.3$ μs and $\tau_\Delta = 3.7$ μs without NaN_3, while $\tau_T = 1.4$ μs and $\tau_\Delta = 3.2$ μs at 0.1 mM of NaN_3. Fitting the data yielded the triplet state quenching rate constant $k_{q,T} = (4.0 \pm 0.2) \times 10^9\ M^{-1}\ s^{-1}$ and the singlet oxygen quenching rate constant $k_{q,\Delta} = (4.6 \pm 0.4) \times 10^8\ M^{-1}\ s^{-1}$. The latter value agrees well with previous literature reports.[38] However, it is important to note that the interpretation of the phosphorescence kinetics of $^1O_2$ in quenching experiments requires caution. We must always be careful whether to attribute the decay time to a singlet oxygen lifetime or to a triplet lifetime.

Our findings confirm the recent results of Ogilby's group obtained in ^3FMN in phosphate buffered D_2O, where the rate constants of triplet quenching of $(3.0 \pm 0.3) \times 10^9\ M^{-1}\ s^{-1}$ and singlet oxygen quenching of $(5.5 \pm 0.3) \times 10^8\ M^{-1}\ s^{-1}$ were measured.[41] Quenching of the flavin chromophore in the miniSOG protein was also previously published.[42]

Remarkably, the high efficiency of NaN_3 in quenching $^3Rf^*$ contrasts with assumptions of many previous studies, which assumed that sodium azide does not quench riboflavin triplets,[21,26–28] although the quenching constant of $3.3 \times 10^9\ M^{-1}\ s^{-1}$ was reported in an older work by Lu *et al.*[43] The paper reported that the quenching proceeds through the reaction $^3Rf^* + N_3^- \rightarrow Rf^{\bullet-} + N_3^\bullet$. This is consistent with considerations based on redox potentials: 1.7 V for the $^3Rf^*/Rf^{\bullet-}$ pair and 1.35 V for the $N_3^-/N_3^\bullet$ pair.[44] Unfortunately, the global analysis of our time-resolved transient absorption spectra (Section 4.1) showed only one spectral and lifetime component corresponding to riboflavin and did not reveal a clear spectral signature of another species such as riboflavin anion, so we are not able to confirm the reported quenching mechanism. Nevertheless, our findings clearly show that NaN_3 is an effective quencher of $^3Rf^*$, and this must be taken into account in future mechanistic interpretations.

4.5 Delayed fluorescence

The time-resolved delayed emission of riboflavin (50 μM in PBS/H_2O) was measured using setup 1 with a 562 nm centred bandpass filter (bandwidth 40 nm). Fig. 4 shows a clear rise-decay profile of

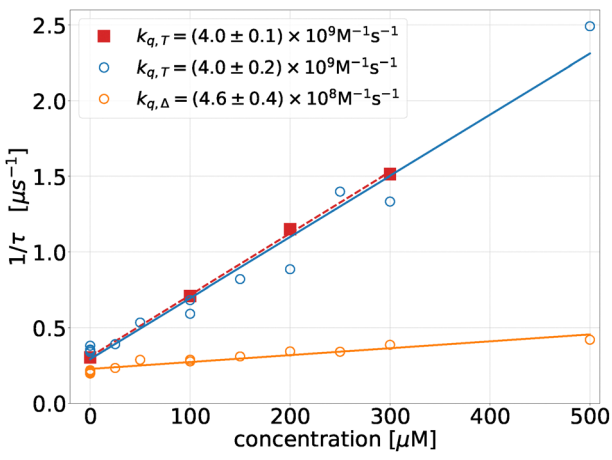

Fig. 3 NaN_3 concentration dependence of the $^1O_2$ deactivation rate (orange open circles) and $^3Rf^*$ deactivation rate obtained from transient absorption (red squares) and from $^1O_2$ phosphorescence (blue open circles).

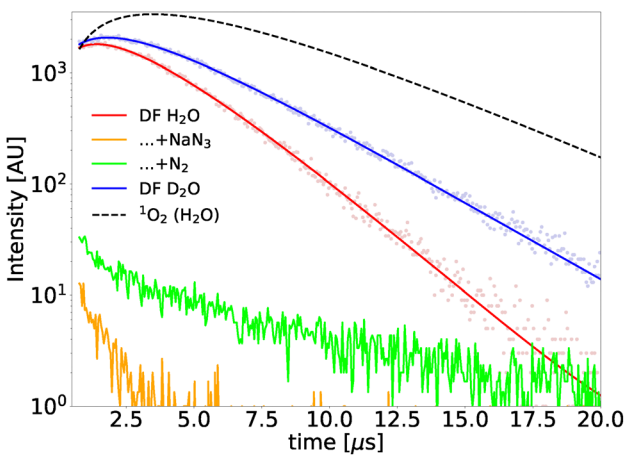

Fig. 4 Kinetics of delayed fluorescence of riboflavin in H_2O (red) and D_2O (blue) with the respective fits of the kinetic model. The signals from the samples where the $^1O_2$ was removed by bubbling with nitrogen (green) or by adding NaN_3 (orange) show no rise-decay behaviour. A fit of the $^1O_2$ phosphorescence kinetics (black, dashed) is added for comparison.

the delayed fluorescence signal. It can be well described by a biexponential fit with a rise time of (1.7 ± 0.1) μs and a decay time of (1.8 ± 0.1) μs. According to the theoretical model of singlet oxygen feedback delayed fluorescence (SOFDF; see eqn (2)), the rise time corresponds to half of the triplet lifetime $\left(\tau_{rise} = \frac{\tau_T}{2}\right)$. This agrees well with τ_T = (3.3 ± 0.1) μs obtained from the rise time of $^1O_2$ phosphorescence. The decay time of the SOFDF is expected to follow eqn (2).[34] For τ_T = 3.3 μs and τ_Δ = 3.7 μs, this yields $\tau_{decay} \approx 1.74$ μs, which closely matches the observed value. These results confirm that the delayed fluorescence kinetics of riboflavin are consistent with the SOFDF mechanism.

Further confirmation of the SOFDF mechanism was obtained by testing the sensitivity of the delayed emission to oxygen. In samples saturated with N_2, the delayed fluorescence signal was quenched by more than 95%, consistent with the singlet oxygen-mediated mechanism.

By adding 10 mM NaN_3, the DF signal was almost completely suppressed, but as previously stated, sodium azide quenches both Rf triplets and $^1O_2$, so this cannot be directly used to prove the participation of $^1O_2$ in the formation of DF. Nevertheless, we measured the DF kinetics at a series of NaN_3 concentrations spanning from 0 to 100 μM, which shortens $^1O_2$ lifetimes only mildly, whereas ^{3}Rf* is significantly quenched. The shortening of the DF lifetimes by azide is clearly visible and is consistent with the SOFDF model, as can be seen in Fig. SI-1 and Table SI-1 in the SI.

We also performed measurements in PBS containing 90% D_2O and 10% H_2O, where the singlet oxygen lifetime is significantly extended. Under such conditions, the SOFDF theory predicts that the rise time remains $\frac{\tau_T}{2}$, while the decay time approaches τ_T. The measured rise and decay times of DF were (1.7 ± 0.1) μs and (2.8 ± 0.1) μs, respectively. Simultaneous singlet oxygen phosphorescence measurements yielded τ_T = 3.4 μs and τ_Δ = 27 μs, which predict SOFDF lifetimes of 1.7 μs and 3.0 μs (eqn (2)). These values agree well with the observed kinetics, further validating the SOFDF interpretation.

The delayed fluorescence spectrum of riboflavin was measured and compared with the prompt fluorescence spectrum using setup no. 3, where a gate window of 0–20 ns captured the prompt fluorescence and a delayed gate window of 1–5 μs captured the delayed fluorescence. The two spectra were practically identical, as shown in Fig. SI-2, which is consistent with our observations on other photosensitizers.[25] The ratio of DF to PF integral intensities was found to be $R \approx 2 \times 10^{-4}$ for riboflavin under our experimental conditions. Our experiments on other sensitisers under similar conditions but with 5× larger absorbances revealed ratios in the order of $R \sim 1 \times 10^{-3}$. Given the second-order dependence of SOFDF on the concentration of excited states, the result in riboflavin is consistent with those observations.

Finally, it should also be noted that no Rf phosphorescence around 620 nm was observed in our liquid samples, even with oxygen removed, contrary to the data reported in solid samples of starch films.[31]

4.6 Energy transfer from Rf to AlPc

Delayed fluorescence (DF) kinetics can serve as a useful tool to investigate energy transfer processes involving the triplet state of riboflavin (^{3}Rf*). Here, we aim to demonstrate that ^{3}Rf* can transfer energy to the ground state of another photosensitiser, aluminium phthalocyanine tetrasulphonate (AlPc), generating its triplet excited state through the reaction:

$$^3\text{Rf}^* + {}^1\text{AlPc} \rightarrow {}^1\text{Rf} + {}^3\text{AlPc}^*, \quad (3)$$

i.e. triplet–triplet energy transfer (TTET), where ^{3}AlPc* subsequently interacts with the surrounding singlet oxygen and emits delayed fluorescence through the SOFDF mechanism.

To investigate this, we prepared solutions of 50 μM riboflavin, 100 μM AlPc, and their equimolar mixture in PBS/H_2O. Using setup 1 with 445 nm excitation (which excites riboflavin efficiently while AlPc absorbs minimally at this wavelength), we simultaneously recorded DF and singlet oxygen phosphorescence. For DF detection, we used either a bandpass filter centred at 690 nm (bandwidth of 40 nm) to isolate AlPc emission or a bandpass filter centred at 562 nm (bandwidth 40 nm) to isolate riboflavin fluorescence. Fig. 5 displays the DF signals of individual samples.

First, DF from riboflavin alone was measured using excitation at 445 nm with detection at 690 nm. As expected, the signal was weak (~500 counts at maximum), as riboflavin does not emit significantly at this wavelength. Similarly, AlPc alone exhibited very weak DF under the same excitation/detection conditions (~300 counts at maximum), as it does not absorb at 445 nm. In contrast, in the mixed solution of riboflavin and AlPc excited at 445 nm, the intensity of DF at 690 nm increased dramatically to ~13 000 counts – more than a 20-fold increase relative to individual components. A similar situation was also observed for a much lower concentration of AlPc (10 μM), see Fig. SI-4. This indicates an efficient energy transfer from ^{3}Rf* to AlPc, which leads to delayed emission from ^{3}AlPc*.

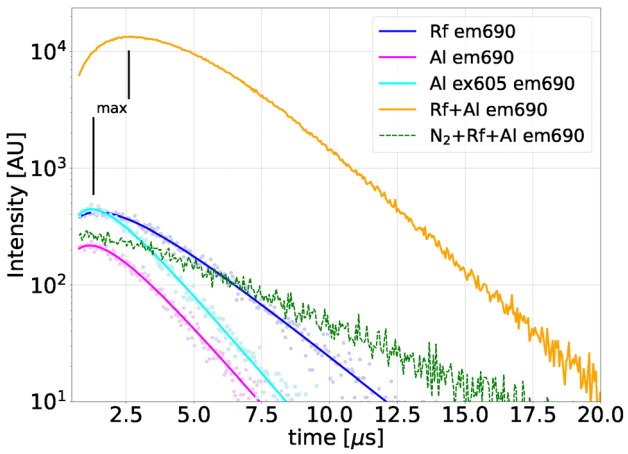

Fig. 5 Delayed fluorescence of samples with Rf (blue) or AlPc (magenta) and their mixture under aerobic (orange) and anaerobic (green) conditions detected at 690 nm with excitation at 445 nm. Delayed fluorescence of the AlPc solution under excitation at 605 nm (cyan) is added for comparison.

To confirm singlet oxygen as an intermediate in the formation of DF in the Rf + AlPc mixture, we repeated the measurement in a nitrogen-saturated sample. In the absence of oxygen, the DF signal at 690 nm was strongly suppressed, indicating that the AlPc emission originates from the SOFDF mechanism, *i.e.* through the interaction between ^{3}AlPc* and $^1O_2$.

However, two alternative pathways of delayed signal formation should be considered:

(a) Formation of ^{1}AlPc* from ^{3}Rf* in a reaction ^{3}Rf* + ^{1}AlPc → ^{1}Rf + ^{1}AlPc* and a subsequent direct emission of delayed fluorescence from ^{1}AlPc* without singlet oxygen as an intermediate.

(b) Singlet–singlet energy transfer (SSET): formation of ^{1}AlPc* from ^{1}Rf* (by FRET, Dexter or emission/reabsorption) and subsequent ISC to ^{3}AlPc* within a few tens of nanoseconds after the excitation pulse, followed by delayed SOFDF emission.

Clearly, pathway (a) can be ruled out based on suppression of the signal in the nitrogen saturated sample, which showed that the SOFDF mechanism took place. The SSET pathway (b) is certainly present along with the proposed TTET mechanism (eqn (3)). If the delayed fluorescence from the mixed Rf and AlPc sample was mainly due to the SSET mechanism, then the DF kinetics should have a shape similar to that of DF from AlPc alone. However, Fig. 5 shows that the delayed signal at 690 nm in the sample with added AlPc has a maximum at a much later time (2.6 μs) than AlPc alone (1.3 μs). The later onset of the delayed signal is consistent with the proposed TTET mechanism (3), where ^{3}AlPc* is formed first by energy transfer from ^{3}Rf*, thus causing the later onset.

Two delayed fluorescence kinetic models were prepared based on independently measured deactivation rates of ^{3}Rf*, $^1O_2$ and ^{3}AlPc*: the first model involves the triplet to triplet energy transfer, while the other model involves only SSET. Fig. 6 clearly shows that the TTET model fits the experimental data quite well, while the SSET model does not.

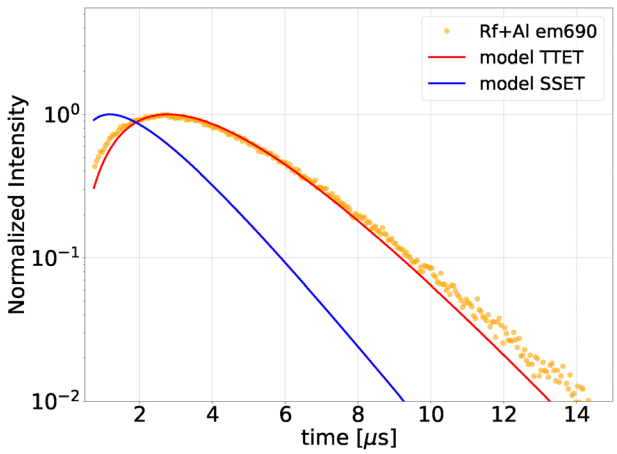

Fig. 6 Delayed fluorescence of AlPc from the mixture of AlPc and riboflavin, excitation at 445 nm and emission detection at 690 nm. Model TTET assumes the triplet to triplet energy transfer from ^{3}Rf*, leading to the formation of ^{3}AlPc*. The SSET model takes into account only the energy transfer from ^{1}Rf*, leading to the formation of ^{1}AlPc*.

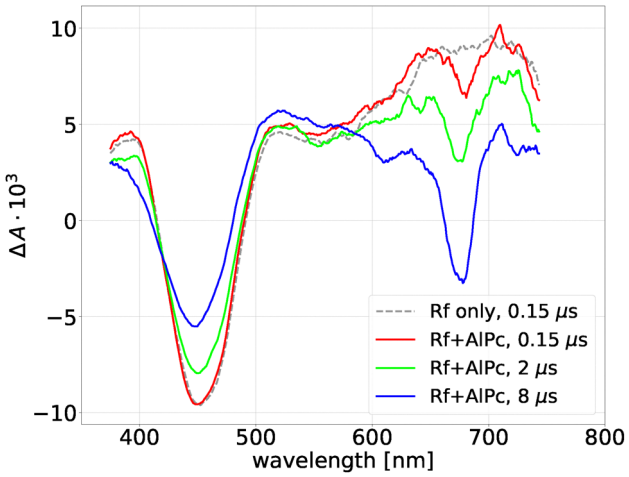

Fig. 7 Energy transfer from ^{3}Rf* to ^{3}AlPc documented by time-resolved transient absorption spectra of riboflavin (50 μM) with AlPc (5 μM) at deoxygenated PBS/H_2O. The riboflavin band around 450 nm decays, while the AlPc band around 670 nm rises with the same time constant of 11 μs. The signature of the AlPc excited state at the short delay (0.15 μs) is only relatively weak which indicates that most of the AlPc excited states are not generated by a singlet–singlet energy transfer, but rather by triplet–triplet energy transfer.

To further support the dominant role of TTET, we performed time-resolved transient absorption measurements on the mixture of Rf (50 μM) and AlPc (5 μM, a lower concentration was needed to keep the absorbance below 1) in a deoxygenated solution. The data showed that the riboflavin band around 450 nm decayed, while the AlPc band around 670 nm increased with the same time constant of 11 μs (Fig. 7), consistent with the TTET mechanism. A relatively weak signature of the AlPc excited state at a short delay (0.15 μs) indicates that the SSET mechanism is only a minor contributor to the formation of AlPc excited states.

Furthermore, the prompt and delayed fluorescence spectra of the samples were measured using setup 2, again with 445 nm excitation. While the intensity of the AlPc delayed fluorescence around 690 nm was dramatically increased in the presence of riboflavin, the prompt fluorescence in the same mixture was only slightly enhanced relative to the individual compounds. The situation is illustrated in Fig. 8 and Fig. SI-3. This further

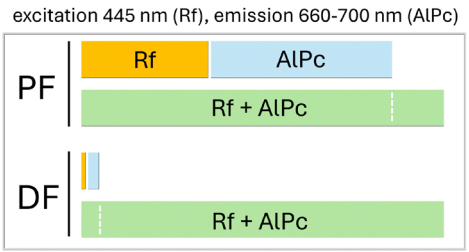

Fig. 8 Delayed fluorescence (DF) and prompt fluorescence (PF) intensity in the 660–700 nm region (AlPc emission), excited at 445 nm (Rf absorption) from AlPc alone, Rf alone, and the mixture of AlPc and riboflavin. Clearly, only DF of AlPc is dramatically enhanced in the presence of riboflavin, which indicates that TTET is dominant and SSET has only a minor effect.

supports the notion that the TTET mechanism (eqn (3)) is the main contributor to the formation of ^{3}AlPc* in our experiment, while SSET has only a minor effect.

Finally, we estimated the rate constant for the energy-transfer reaction. Analysis of riboflavin DF decay at 562 nm revealed the ^{3}Rf* lifetime of $\tau_T = (3.3 \pm 0.3)$ μs in the absence of AlPc (calculated using eqn (2)). Upon the addition of 100 μM AlPc, the lifetime of ^{3}Rf* decreased to $\tau'_T = (2.4 \pm 0.2)$ μs, see Fig. 9. The corresponding increase in the triplet decay rate is

$$K_q = \frac{1}{\tau_T} - \frac{1}{\tau'_T} \approx 1.1 \times 10^5\ \mathrm{s}^{-1}. \quad (4)$$

This gives an estimated bimolecular quenching rate constant of

$$k_q = \frac{K_q}{[\mathrm{AlPc}]} = \frac{1.1 \times 10^5\ \mathrm{s}^{-1}}{1 \times 10^{-4}\ \mathrm{M}} = 1.1 \times 10^9\ \mathrm{M}^{-1}\ \mathrm{s}^{-1}. \quad (5)$$

Although approximate, this estimate illustrates how DF measurements can be applied to investigate triplet-state quenching and energy transfer dynamics between photosensitisers. Compared with the transient absorption technique for investigations of energy transfer, delayed fluorescence provides a background-free method with the possibility of faster data acquisition. Here, we also see that delayed fluorescence enabled us to investigate samples with relatively larger concentrations of AlPc, whereas the pump–probe transient absorption at a right-angle geometry was limited to much smaller concentrations because of the large absorption coefficients of AlPc. However, delayed fluorescence signal interpretation could be more complicated because additional influences may be present.

As an example, delayed fluorescence was previously used to investigate triplet–triplet energy transfer in pyrene doped phenanthrene nanoparticles, where pyrene acted as an energy acceptor and emitted DF likely by a triplet–triplet annihilation upconversion mechanism.[45] However, such use cases for LED and lighting applications are quite distant from our biologically relevant systems.

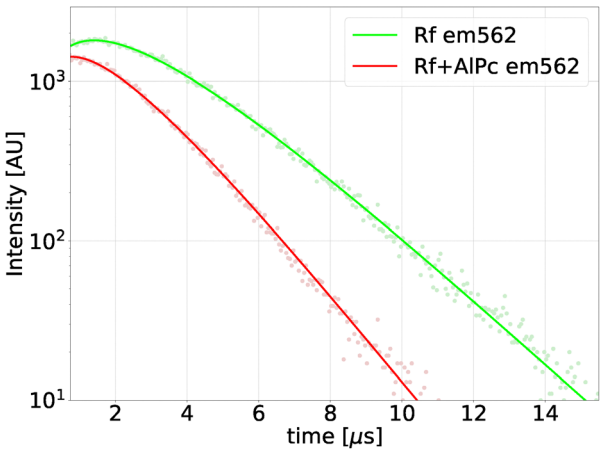

Fig. 9 Riboflavin delayed fluorescence excited at 445 nm and emission detected at the Rf fluorescence wavelength of 562 nm without AlPc (green) and in the presence of 100 μM AlPc (red). We can clearly see the quenching of ^{3}Rf* in the presence of AlPc.

Conclusions

This study provides a detailed investigation of the triplet state and the photophysical behaviour of riboflavin in aqueous media. We confirmed that the triplet lifetime of riboflavin in PBS/H_2O is approximately 3.2 μs, being close to the singlet oxygen lifetime of ~3.7 μs, which presents challenges for the kinetic analysis of the emission of $^1O_2$. To address this, we combined independent methods to evaluate the triplet lifetimes: transient absorption and singlet oxygen luminescence. We confirmed that riboflavin is a poor quencher of singlet oxygen in H_2O, with a bimolecular rate constant below 6×10^7 M^{-1} s^{-1}, supporting recent findings obtained in D_2O that contradict previous assumptions of efficient quenching. Given the low solubility of riboflavin in water (<200 μM), the overall $^1O_2$ quenching rate is negligible compared to that of other deactivation pathways. Furthermore, we confirmed that sodium azide, commonly considered a selective quencher of singlet oxygen, very efficiently quenches the triplet state of riboflavin ($k_q \approx 4 \times 10^9$ M^{-1} s^{-1}), with significant implications for the interpretation of previous studies. We also report the first observation of singlet oxygen feedback delayed fluorescence (SOFDF) in riboflavin, with kinetics consistent with the expected model in both H_2O and D_2O. SOFDF was a dominant mode of delayed emission in our samples. This provides a new experimental tool to probe the excited-state dynamics of riboflavin. Finally, we demonstrate that delayed fluorescence measurements can be used to study triplet–triplet energy transfer, as evidenced by riboflavin transferring energy to aluminium phthalocyanine in solution. Together, our results clarify several longstanding ambiguities about the behaviour of the triplet state of riboflavin and highlight important considerations for future studies involving flavin-based photosensitisers in biological, environmental, or photodynamic contexts.

Author contributions

Marek Scholz: conceptualization, methodology, investigation, formal analysis, visualization, writing – original draft preparation, and writing – review and editing. Jan Moučka: investigation and formal analysis. Jakub Pšenčík: investigation and formal analysis. Jan Hála: conceptualization, methodology, formal analysis, writing – original draft preparation, and writing – review and editing. Roman Dědic: conceptualization, methodology, data curation, investigation, formal analysis, visualization, writing – original draft preparation, and writing – review and editing.

Conflicts of interest

There are no conflicts to declare.

Data availability

The data presented in the study are publicly available in the Zenodo repository (DOI: https://doi.org/10.5281/zenodo.17288541). The raw experimental data supporting the findings of this study, simulation input files, output data, and analysis scripts are available from the corresponding author upon request.

Supplementary information (SI) is available. See DOI: https://doi.org/10.1039/d5cp03884g.

References

1 N. Suwannasom, I. Kao, A. Pruß, R. Georgieva and H. Bäumler, *Int. J. Mol. Sci.*, 2020, **21**, 950.
2 M. Insińska-Rak, M. Sikorski and A. Wolnicka-Glubisz, *Cells*, 2023, **12**, 2304.
3 D. R. Cardoso, S. H. Libardi and L. H. Skibsted, *Food Funct.*, 2012, **3**, 487–502.
4 K. Huvaere and L. H. Skibsted, *J. Food Agric.*, 2015, **95**, 20–35.
5 M. Westberg, L. Holmegaard, F. M. Pimenta, M. Etzerodt and P. R. Ogilby, *J. Am. Chem. Soc.*, 2015, **137**, 1632–1642.
6 M. Westberg, M. Bregnhøj, M. Etzerodt and P. R. Ogilby, *J. Phys. Chem. B*, 2017, **121**, 2561–2574.
7 C. Lafaye, S. Aumonier, J. Torra, L. Signor, D. von Stetten, M. Noirclerc-Savoye, X. Shu, R. Ruiz-González, G. Gotthard, A. Royant and S. Nonell, *Photochem. Photobiol. Sci.*, 2022, **21**, 1545–1555.
8 J. N. Chacon, J. McLearie and R. S. Sinclair, *Photochem. Photobiol.*, 1988, **47**, 647–656.
9 J. Baier, T. Maisch, M. Maier, E. Engel, M. Landthaler and W. Bäumler, *Biophys. J.*, 2006, **91**, 1452–1459.
10 F. M. Pimenta, R. L. Jensen, T. Breitenbach, M. Etzerodt and P. R. Ogilby, *Photochem. Photobiol.*, 2013, **89**, 1116–1126.
11 M. Ohara, T. Fujikura and H. Fujiwara, *Int. J. Oncol.*, 2003, **22**, 1291–1295.
12 E. V. Khaydukov, K. E. Mironova, V. A. Semchishen, A. N. Generalova, A. V. Nechaev, D. A. Khochenkov, E. V. Stepanova, O. I. Lebedev, A. V. Zvyagin, S. M. Deyev and V. Y. Panchenko, *Sci. Rep.*, 2016, **6**, 35103.
13 R. A. Akasov, N. V. Sholina, D. A. Khochenkov, A. V. Alova, P. V. Gorelkin, A. S. Erofeev, A. N. Generalova and E. V. Khaydukov, *Sci. Rep.*, 2019, **9**, 9679.
14 H. M. Faddy, J. J. Fryk, D. Watterson, P. R. Young, N. Modhiran, D. A. Muller, S. D. Keil, R. P. Goodrich and D. C. Marks, *Vox Sang.*, 2016, **111**, 235–241.
15 K. Makdoumi, R. Goodrich and A. Bäckman, *Acta Ophthalmol.*, 2017, **95**, 498–502.
16 D. Ortega-Zambrano, D. Fuentes-López and H. Mercado-Uribe, *J. Innovative Opt. Health Sci.*, 2022, **15**, 2240010.
17 P. V. Krikunova, E. R. Tolordava, N. A. Arkharova, D. N. Karimov, T. V. Bukreeva, V. Z. Shirinian, E. V. Khaydukov and T. N. Pallaeva, *ACS Appl. Mater. Interfaces*, 2024, **16**, 5504–5512.
18 N. Ulmann, J. Hioe, D. Touraud, D. Horinek and W. Kunz, *Phys. Chem. Chem. Phys.*, 2024, **26**, 18930–18942.
19 M. Insińska-Rak, P. Henke, T. Breitenbach and P. R. Ogilby, *J. Photochem. Photobiol., A*, 2024, **446**, 115108.
20 M. A. Sheraz, S. H. Kazi, S. Ahmed, Z. Anwar and I. Ahmad, *Beilstein J. Org. Chem.*, 2014, **10**, 1999–2012.
21 R. Huang, E. Choe and D. Min, *J. Food Sci.*, 2004, **69**, C726–C732.
22 R. Huang, H. J. Kim and D. B. Min, *J. Agric. Food Chem.*, 2006, **54**, 2359–2364.
23 S. Yang, J. Lee, J. Lee and J. Lee, *Food Chem.*, 2007, **105**, 1375–1381.
24 L. Costa, M. A. F. Faustino, J. P. C. Tomé, M. G. P. M. S. Neves, A. C. Tomé, J. A. S. Cavaleiro, A. Cunha and A. Almeida, *J. Photochem. Photobiol., B*, 2013, **120**, 10–16.
25 M. Scholz, R. Dědic, T. Breitenbach and J. Hála, *Photochem. Photobiol. Sci.*, 2013, **12**, 1873–1884.
26 M. Díaz, M. Luiz, S. Bertolotti, S. Miskoski and N. A. García, *Can. J. Chem.*, 2004, **82**, 1752–1759.
27 M. Y. Jung, Y. S. Oh, D. K. Kim, H. J. Kim and D. B. Min, *J. Agric. Food Chem.*, 2007, **55**, 170–174.
28 K. Hirakawa and T. Yoshioka, *Chem. Phys. Lett.*, 2015, **634**, 221–224.
29 F. Wilkinson, W. P. Helman and A. B. Ross, *J. Phys. Chem. Ref. Data*, 1995, **24**, 663–1021.
30 M. Bregnhøj, M. Westberg, F. Jensen and P. R. Ogilby, *Phys. Chem. Chem. Phys.*, 2016, **18**, 22946–22961.
31 A. Penzkofer, *Chem. Phys.*, 2012, **400**, 142–153.
32 M. Scholz, R. Dědic, J. Hála and S. Nonell, *J. Mol. Struct.*, 2013, **1044**, 303–307.
33 I. S. Vinklárek, M. Scholz, R. Dědic and J. Hála, *Photochem. Photobiol. Sci.*, 2017, **16**, 507–518.
34 M. Scholz and R. Dědic, *Singlet Oxygen: Applications in Biosciences and Nanosciences*, Royal Society of Chemistry, London, 2016, ch. 28, vol. 14, pp. 63–81.
35 I. H. M. van Stokkum, D. S. Larsen and R. van Grondelle, *Biochim. Biophys. Acta, Bioenerg.*, 2004, **1657**, 82–104.
36 T. B. Melø, M. A. Ionescu, G. Haggquist and K. R. Naqvi, *Spectrochim. Acta, Part A*, 1999, **55**, 2299–2307.
37 Z. Kvíčalová, J. Alster, E. Hofmann, P. Khoroshyy, R. Litvín, D. Bína, T. Polívka and J. Pšenčík, *Biochim. Biophys. Acta, Bioenerg.*, 2016, **1857**, 341–349.
38 R. D. Hall and C. F. Chignell, *Photochem. Photobiol.*, 1987, **45**, 459–464.
39 A. Michaeli and J. Feitelson, *Photochem. Photobiol.*, 1994, **59**, 284–289.
40 M. Scholz, R. Dědic, A. Svoboda and J. Hála, *J. Mol. Struct.*, 2011, **993**, 474–476.
41 M. Bregnhøj, F. Thorning and P. R. Ogilby, *Chem. Rev.*, 2024, **124**, 9949–10051.
42 T.-L. To, M. J. Fadul and X. Shu, *Nat. Commun.*, 2014, **5**, 4072.
43 C. Lu, Z. Han, G. Liu, X. Cai, Y. Chen and S. Yao, *Sci. China, Ser. B:Chem.*, 2001, **44**, 39–48.
44 Z. B. Alfassi, A. Harriman, R. E. Huie, S. Mosseri and P. Neta, *J. Phys. Chem.*, 1987, **91**, 2120–2122.
45 Z. Jiang, Y. Zhao, Z. Luo, A. Peng, H. Wang and J. Yao, *Chin. J. Chem.*, 2010, **28**, 2103–2108.